Polyhedron 47 (2012) 53–59

Contents lists available at SciVerse ScienceDirect

Polyhedron

journal homepage: www.elsevier.com/locate/poly

Structure and magnetism of catena-poly[copper(II)-μ-dichloro-L-lysine]hemihydrate: Copper chains with monochloride bridges

Ricardo C. Santana [a,*], Bruno N. Ferreira [a], José R. Sabino [a], Jesiel F. Carvalho [a], Octavio Peña [b], Rafael Calvo [c]

[a] Instituto de Física, Universidade Federal de Goiás, Campus Samambaia, CP 131, 74001-970 Goiânia (GO), Brazil
[b] UMR 6226 CNRS, Institut des Sciences Chimiques de Rennes, Université de Rennes 1, 35042 Rennes, France
[c] Facultad de Bioquímica y Ciencias Biológicas, Universidad Nacional del Litoral, and INTEC (CONICET-UNL), Güemes 3450, 3000 Santa Fe, Argentina

ARTICLE INFO

Article history:
Received 10 July 2012
Accepted 20 August 2012
Available online 30 August 2012

Keywords:
Copper
Lysine
Structure
Chlorine bridge
Exchange interaction
Magnetic properties
EPR spectra

ABSTRACT

We report the preparation and characterization by elemental analysis, infrared (IR), single crystal X-ray diffraction, magnetic measurements and electron paramagnetic resonance (EPR) of the new compound catena-poly[copper(II)-μ-dichloro-L-lysine]hemihydrate, with formula $C_6H_{14}Cl_2CuN_2O_2\cdot(H_2O)_{0.5}$, here after called [Cu(lys)Cl_2]. The compound crystallizes in the space group C2 with copper ions in a square pyramidal coordination, and the structure consists of zigzag chains along the ***b*** axis bridged by equatorial-apical chlorine bonds with Cu–Cu distance of 3.5414(4) Å, and a small Cu–Cl–Cu angle of 85.47(6)°. Magnetic susceptibility and isothermal magnetization curves reveals a weak antiferromagnetic interaction $2J = -0.30(2)$ cm^{-1} supported by the Cu–Cl–Cu bridge connecting Cu^{II} neighbors in the chains. EPR spectra at 34.0 GHz were obtained in powdered samples and in a single crystal with $\boldsymbol{B}_0$ in three orthogonal planes. Assuming an axially symmetric molecular ***g***-matrix, we obtained principal *g*-values $g_{//} = 2.2794(9)$ and $g_{\perp} = 2.0489(3)$ from the crystal *g*-matrix calculated using the observed angular variation of the EPR line position. The angular variation of the line width, largest along the chain direction, is attributed to dipolar couplings between Cu^{II} ions in the lattice. The magnetic and EPR results are discussed in terms of the exchange couplings.

1. Introduction

Metal-amino acid compounds are appropriate model systems of biomolecules to investigate the molecular and electronic structure of metal ions in protein-like structures [1] and the exchange interactions transmitted through the chemical paths connecting the unpaired spins [2]. As copper is an abundant bioelement providing active sites to several metalloenzymes and proteins [3–6], many efforts have been oriented to study copper amino acid complexes [7]. Also, several copper(II)-amino acid complexes have been shown to display a spin-chain behavior [8]. L-Lysine is one of three basic amino acids and has a positive charge on its side-chain at pH 7.0, favouring the formation of metal complexes [9].

Since the early work of Dunitz [10], compounds containing Cu^{II} motifs connected by one [11–20] or two [21–25] chloride bridges have been reported. In chain compounds one-chloride bridges may connect equatorial and apical positions, with Cu–Cl–Cu angles varying from 80 to 180°. Magnetic studies and magneto structural analyses in these compounds [11–20] have gained attention in the field of magnetism [26–28], and since the works of Willet et al. [29] and Hatfield et al. [30–32], efforts have been directed to relate the exchange coupling $2J$ ($\mathcal{H}_{ex}(i, i+1) = -2J_{i,i+1}\boldsymbol{S}_i\cdot\boldsymbol{S}_{i+1}$), as generally defined for chain compounds [33]), with the structural features such as Cu–Cl–Cu bond angles, and Cu···Cu and Cu–Cl distances describing the chloro-bridged Cu^{II} motifs [28,29,34].

In this work we have studied the new copper compound catena-poly[copper(II)-μ-dichloro-L-lysine]hemihydrate, here after called [Cu(lys)Cl_2], exhibiting chains of copper ions connected by chlorine bridges with an unusually small Cu–Cl–Cu bond angle. We synthesized the compound, solved the crystal structure, and performed magnetic and EPR studies, with the aim to investigate the electronic properties of the Cu molecules, and the magnetic interactions between neighbor Cu^{II} ions in the chains. The magneto structural correlations of the Cu–Cl–Cu equatorial-apical bond are discussed.

2. Experimental

2.1. Synthesis

2.1.1. Materials

The reagents and solvents were used as received without further purification and all experiments were carried out in open atmosphere. The L-lysine hydrochloride ($C_6H_{14}N_2O_2\cdot HCl$) and copper nitrate trihydrate ($Cu(NO_3)_2\cdot 3H_2O$) used for the synthesis were

* Corresponding author. Tel./fax: +55 62 3521 1014.
E-mail address: santana@if.ufg.br (R.C. Santana).

0277-5387/$ - see front matter © 2012 Elsevier Ltd. All rights reserved.
http://dx.doi.org/10.1016/j.poly.2012.08.045

commercially available from Ajinomoto Co. and Synth Co., respectively.

2.1.2. [Cu(lys)Cl_2]

Crystals of [Cu(lys)Cl_2] were grown by precipitation from water or ethanol solutions of 1:1 molar ratios of L-lysine·HCl, and $Cu(NO_3)_2{\cdot}3H_2O$. The aqueous solution was prepared by mixing 55.75 g of L-lysine·HCl and 73.71 g of copper nitrate trihydrate in 50 ml of distilled water. The mixture was heated to about 50 °C while vigorously stirred, and after few minutes a clear and homogeneous solution with intense blue coloration was obtained. The solution was allowed to evaporate slowly at 24 °C and few crystals precipitated after 2 months. Alcoholic solutions were prepared by adding 0.500 g of L-lysine·HCl and 0.613 g of copper nitrate trihydrate to 500 ml of ethanol 99.5%, heated to 50 °C and stirred during about 5 h until the complete dissolution of the solutes; the alcohol was allowed to evaporate slowly at 24 °C, and after few days microcrystals were obtained from the clear bluish solution. L-lysine·HCl is highly soluble in water and the viscosity of the solution is large during the crystallization, making difficult the mass transport process and requiring long time for nucleation and growth. On the other hand, the solubility of the compound in ethanol is low, the solvent evaporation does not cause a significant increase in the solution viscosity, and crystals can be obtained after few days. The growth habit of the crystals obtained using both solvents are similar, they display an acicular morphology elongated along the ***b*** axis and well defined prismatic faces. The crystals grown from aqueous solution have dimensions up to about $2 \times 0.3 \times 0.2$ mm^3 while the dimensions of those from alcoholic solutions are few microns. X-ray diffraction measurements demonstrated that crystals grown from both solutions have the same crystal structure. *Anal.* Calc. for $C_6H_{14}Cl_2CuN_2O_2(H_2O)_{0.50}$: C, 24.9; H, 5.2; N, 9.7; Cu, 21.9. Found: C, 24.3; H, 4.6; N, 9.9; Cu, 22.0%.

2.2. Methods

Crystal composition was investigated by elemental analysis of CNH performed on a Perkin Elmer series II 2400 analyzer, and Cu^{II} content by optical emission spectroscopy on a Perkin Elmer 3000 DV. IR spectra were recorded on a Nicolet 510P FT-IR spectrophotometer using [Cu(lys)Cl_2] powder diluted in KBr pellets.

Magnetic measurements were performed with a Quantum Design Squid magnetometer MPMS XL5 using calibrated gelatine capsules as sample holders having a small diamagnetic contribution and containing 78.2 mg of powdered [Cu(lys)Cl_2]. The magnetic susceptibility was measured in the temperature (T) range between 2 and 280 K, under a magnetic field $B_0 = \mu_0 H = 0.1$ T (μ_0 is the permeability of the vacuum). A magnetization isotherm was measured at 2 K with B_0 between 0 and 5 T.

EPR measurements were performed at 300 K in an ESP-300 Bruker spectrometer working at 34.0 GHz (Q-band), with a standard Bruker ER5101Q cylindrical cavity operating with 100 kHz magnetic field modulation, and a rotating magnet. The sample orientation was attained by gluing the *ab* growth face to a cleavage face of a KBr single crystal cubic holder defining a system ***xyz*** of orthogonal axes, with ***x*** ≡ ***a***, ***y*** ≡ ***b***, ***z*** ≡ ***c**** (***c**** = ***a*** × ***b***). This sample holder was mounted on top of a rexolite pedestal inside of the microwave cavity, and the spectra were recorded at 5° orientation intervals of the external magnetic field, in ranges of 180° of the *ab*, *bc** and *ac** planes, at 300 K. The magnetic field at the position of the sample was calibrated using DPPH ($g = 2.0036$) as field marker. Positions and peak-to-peak line widths (ΔB_{PP}) of the resonance were obtained by least-squares fitting of the spectra to Lorentzian derivative line shapes. The positions of the ***b*** axis in the *ab* and *bc** planes were determined within 1° from the symmetry properties of the angular variation of the *g*-value.

2.3. Crystallographic data collection and structure refinements

A needle shaped single crystal of [Cu(lys)Cl_2] was mounted on an Enraf–Nonius KappaCCD diffractometer [35] using graphite-monochromated Mo Kα radiation ($\lambda = 0.71073$ Å) at room temperature. Diffraction data were acquired in φ–ω scan mode using the Bruker–Nonius COLLECT package [36] and the raw data processing was carried out with HKL Denzo–Scalepack [37]. Absorption correction was conducted using the indexed crystal faces and Gaussian quadrature methods [38]. The structure was solved using direct methods with SHELXS-97 [39] and the refinements were performed by full-matrix least squares on F^2 with SHELXL-97 [40]. Non-hydrogen atoms were refined anisotropically and hydrogen atoms were positioned geometrically and refined with riding constraints to their parent atoms. The water molecule hydrogen atom H31 was located in the density map and fixed. Art-work representations were prepared using ORTEP-3 [41] and MERCURY [42] from the suite of programs WINGX [43]. Details of the crystallographic and refinement data are given in Table 1.

3. Experimental results

3.1. Spectroscopic results of [Cu(lys)Cl_2]

The IR spectrum, not shown here for brevity, is consistent with the structural results. The NH_2 wagging mode was observed at 1585 cm^{-1} as a sharp shoulder of the intense −COO asymmetric stretching mode band at 1628 cm^{-1}, confirming the complex formation and the covalent bonding to copper. Characteristic stretching modes of the NH_2 group appear at ∼3294, ∼3242 and ∼3134 cm^{-1}. A band at 603 cm^{-1} is attributed to asymmetric vibration of Cu–N [44,45]. Other observed infrared bands are, 1504 cm^{-1} $-NH_3^+$ symmetric deformation, 1406 cm^{-1} $-CH_2$ scissor, 2935 cm^{-1} −C−H asymmetric stretching, 542 cm^{-1} $-COO^-$ wagging, 753 cm^{-1} $-COO^-$ scissor, 801 cm^{-1} $-CH_2$ rocking, 1341 cm^{-1} CH_2 twist [46].

Table 1
Crystal data and structure refinement for [Cu(lys)Cl_2].

Empirical formula	$C_6H_{14}Cl_2CuN_2O_2{\cdot}(H_2O)_{0.5}$
Formula weight	289.65
Temperature	298(2) (K)
Wavelength	0.71073 (Å)
Crystal system	monoclinic
Space group	C2 (N° 5)
Unit cell dimensions	
$a = 20.8260(11)$ (Å)	$\alpha = 90.0(1)$ (°)
$b = 5.8170(2)$ (Å)	$\beta = 104.831(3)$ (°)
$c = 9.4980(5)$ (Å)	$\gamma = 90.0(1)$ (°)
V	1112.30(9) (Å^3)
Z	4
D_{calc}	1.73 (Mg/m^3)
Absorption coefficient	2.422 (mm^{-1})
$F(000)$	592
Crystal size (mm), colour	$0.35 \times 0.05 \times 0.05$, blue
Index ranges	$-25 \leqslant h \leqslant 26$, $-5 \leqslant k \leqslant 7$, $-12 \leqslant l \leqslant 12$
Reflections collected	6995
Independent reflections (R_{int})	2368 (0.045)
Max. and min. transmission	0.904 and 0.685
Refinement method	full matrix least squares on F^2
Data/restraints/parameters	2366/9/138
Goodness-of-fit (GOF) on F^2	1.04
Final R indices [$I > 2\sigma(I)$]	$R_1 = 0.042$, $wR_2 = 0.1037$
R indices (all data)	$R_1 = 0.0656$, $wR_2 = 0.117$
Absolute structure parameter	−0.026(19)
Extinction coefficient	0.025(3)
Largest difference peak and hole	0.57 and −0.77 (e Å^{-3})

3.2. Crystallographic results for [Cu(lys)Cl_2]

An ORTEP view of the asymmetric unit of [Cu(lys)Cl_2] is depicted in Fig. 1, and the selected bond lengths and angles are listed in Table 2.

The Cu^{II} ions are in a square pyramidal coordination, equatorially bonded to the amine N1, one carboxylate O1 atom from a L-lysine molecule, and to two Cl anions, Cl1 and Cl2. A Cl2 atom of a neighboring molecule is at the apex of the pyramid. The angles N1–Cu–Cl1 and O1–Cu–Cl2 are 178.01(17)° and 171.29(13)°, respectively. The equatorial distances are comparable with average literature values but the apical Cu–$Cl2_{ap}$ distance is longer than commonly observed for polymeric Cu^{II} complexes [10,11,15–17,19,20]. The displacement of the copper ion from the basal plane, away from the apical ligand, is 0.04 Å. The geometry around Cu^{II} is consistent with a strongly distorted five coordinate stereochemistry [11–16], usually presenting either a square pyramidal (SP), trigonal bipyramidal (TBP) geometry or intermediate situations. The degree of distortion parameter τ defined by Addison et al. [47] and Hathaway et al. [48] as $(\beta-\alpha)/60$, where β and α are the largest Cu^{II} coordination angles, with values 1 and 0 for ideal TBP and SP, respectively, is here $\tau = 0.11$, suggesting a distorted SP geometry.

Fig. 2 displays the packing of the four symmetry-related molecules in the unit cell, labeled A, B, C and D, showing the bridge –Cu–Cl2–Cu– connecting neighbor Cu^{II} ions at a distance of 3.5414(4) Å inside a chain, with total path length $d = 5.1812$ Å. The angles Cl1–Cu–Cl2 and Cu–Cl2–Cu (see Table 2) and the angle 2.27° between the normal to the equatorial planes of CuA and CuD, are relevant to the exchange interaction between Cu^{II} ions and thus to the magnetic and EPR results. The acute Cu–Cl2–Cu angle is uncommon in compounds with monochloride bridges (see Table 5 in ref. [17] and Table 3 in ref. [19], where this angle varies between 98° and 145°), and an important characteristic of [Cu(lys)Cl_2].

The structure consists of zigzag polymeric linear chains parallel to the ***b*** axis, formed by monomer units linked by equatorial–apical chloride bridges. Neighbor chains interact through electrostatic forces due to the zwitterions of the amino acid; further crystal stabilization is due to hydrogen bonds mediated by the water molecule, which is positioned in the 2-fold axis at (½, *y*, ½), through the amine and carboxylate moieties. The water molecule behaves as hydrogen donor in the interaction O3–H31A···O1, and as hydrogen acceptor in the interaction N12–H12C···$O3^{i}$. An additional H-bond involving the amine atom N12–H12A···$O2^{v}$ helps stabilizing the structure (symmetry codes: (i) as in the caption of Fig. 3; (v) $1-x, -1+y, 2-z$). The water molecules in the 2-fold axis create an interaction path CuA–O1A···H3A–O3–H3B···O1B–CuB connecting CuA to CuB separated by 8.394 Å, having a total length of 9.914 Å. The chemical paths connecting a CuA to a neighbor CuD (or CuB to CuC) in the same chain are much stronger than the paths connecting CuA to the more distant CuB and CuC in neighbor chains. Consequently, the magnitude $|J_{AD}|$ of the exchange interaction between these Cu^{II} ions is expected to be much larger than the exchange interactions $|J_{AB}|$ and $|J_{AC}|$. This result allows interpreting the magnetic and EPR data in terms of Cu^{II} spin chains along the ***b*** axis.

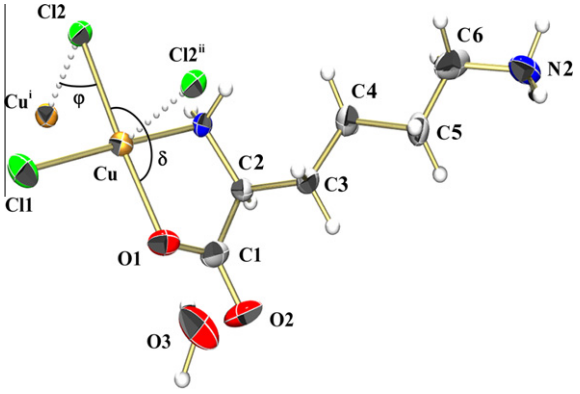

Fig. 1. ORTEP drawing of the asymmetric unit of [Cu(lys)Cl_2] including the labeling scheme. Atom displacement ellipsoids are drawn at the 30% probability level. Hydrogen atoms are shown as spheres of arbitrary radii. Symmetry operations are: (i) $1/2-x, 1/2+y, 1-z$; (ii) $1/2-x, -1/2+y, 1-z$.

Table 2
Selected bond lengths (Å) and angles (°) for [Cu(lys)Cl_2]. *Symmetry operations:* (i) $1/2-x, -1/2+y, 1-z$; (ii) $1/2-x, 1/2+y, 1-z$.

Cu–O1	1.984(3)	O1–Cu–N1	83.91(15)
Cu–N1	1.986(3)	O1–Cu–Cl1	95.01(12)
Cu–Cl1	2.2594(12)	N1–Cu–$Cl2_{eq}$	88.99(10)
Cu–$Cl2_{eq}$	2.3022(11)	N1–Cu–Cl1	178.01(18)
Cu–$Cl2_{ap}$	2.879(2)	Cl1–Cu–$Cl2_{eq}$	91.94(5)
O1–C1	1.271(7)	O1–Cu–$Cl2_{eq}$	171.29(13)
N1–C12	1.457(6)	C12–N1–Cu	111.5(3)
O3–N2	2.925(7)	Cl2 eq–Cu–$Cl2_{ap}^{i}$	97.24(6)
C3–O1	2.929(5)	Cu–Cl2–CuII	85.48(6)

3.3. Magnetic properties

The symbols in Fig. 3a, b display the observed molar susceptibility χ_M vs. T for [Cu(lys)Cl_2] and the molecular magnetization $M(B_0, T)/N_{Av}$ measured at 2 K in a field range between $B_0 = 0$ and 5 T. The contributions of the sample holder, the diamagnetism and temperature independent paramagnetism of the sample are already subtracted from the data.

The magnetic susceptibility and magnetization for linear chain Cu^{II} compounds with nearest neighbor Heisenberg exchange coupling $\mathcal{H}_{ex}(i, i+1) = -2J\,\boldsymbol{S_i}\cdot\boldsymbol{S_{i+1}}$ was modeled following Bonner and Fisher [33], extrapolating to infinite chains the properties calculated numerically for finite chains. Under an applied field $\boldsymbol{B}_0$ along ***z***, and assuming isotropic *g*-factors, finite chains are described by:

$$\mathcal{H} = -2J\sum_{i}^{N_s}\boldsymbol{S}_i\cdot\boldsymbol{S}_{i+1} + g\mu_B B_0\sum_{i}^{N_s}S_{iz} \tag{1}$$

where periodic conditions $\boldsymbol{S}_{N_s+1} = \boldsymbol{S}_1$ are imposed. The molar magnetization and the susceptibility can be written as [49,50]:

$$M(B_0, T) = -\frac{N_{Av}g\mu_B < S_z >}{N_s} \tag{2}$$

and,

$$\chi_M(x) = \frac{N_{Av}g^2\mu_B^2}{N_s x|J|}[< S_z^2 > - < S_z >^2] \tag{3}$$

where N_{Av} is the Avogadro's number, $<S_z>$ and $< S_z^2 >$ are thermal averages of S_z and S_z^2 calculated for a spin chain with N_s spins under B_0 at temperature T ($<S_z> \sim 0$ at low B_0), and $x = k_BT/|J|$ is the reduced temperature. Eigenvalues and thermodynamic properties for chains of up to 20 spins ½ have been reported [33,50,51]. For simplicity we chose the approximate results given by Hall et al. [52] (calculated with chains of up to 11 spins) and by Sartoris et al. [53] (calculated with chains of up to 16 spins):

$$\chi_M(x) = \frac{N_{Av}g^2\mu_B^2}{|J|}\kappa(x) \tag{4}$$

with [53]:

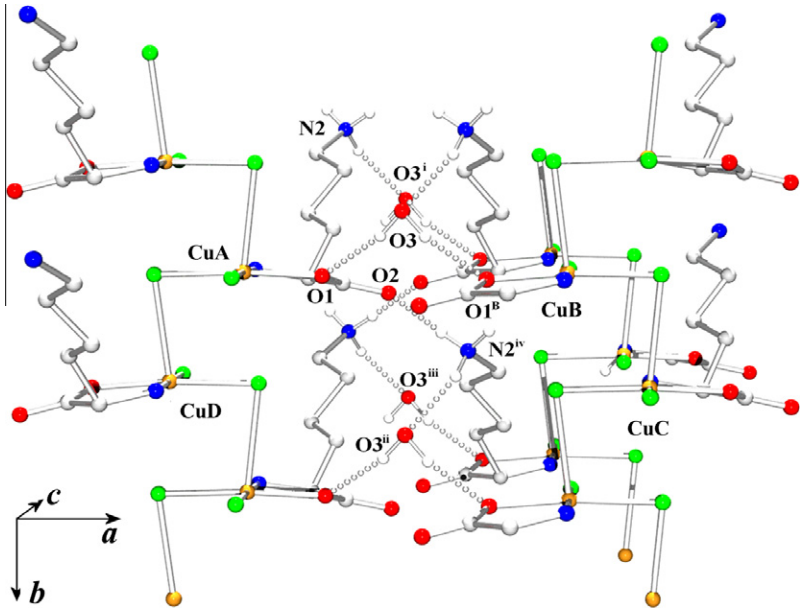

Fig. 2. Crystal packing showing of the Cu chains in the structure of $[Cu(lys)Cl_2]$. Some atoms are omitted for clarity. Dotted lines are hydrogen bonds connecting parallel linear chains. Symmetry operations are: (i) $x, y, 1+z$; (ii) $x, 1+y, z$; (iii) $x, 1+y, 1+z$; (iv) $1-x, 1-y, 2-z$.

Table 3
Components of the crystal g^2 matrix obtained by least squares fits of the function $g^2(\theta, \phi) = \boldsymbol{h}.\boldsymbol{g}.\boldsymbol{g}.\boldsymbol{h}$ to the experimental values at 34.0 GHz displayed in Fig. 4a. $(g^2)_1$, $(g^2)_2$, $(g^2)_3$ and $\boldsymbol{a_1}, \boldsymbol{a_2}, \boldsymbol{a_3}$ are the eigenvalues and eigenvectors of this matrix. $g_\perp$ and $g_{//}$ were calculated for the molecular $\boldsymbol{g}$ matrix of the Cu^{II} ions assuming axial symmetry. We include the angles (θ_m, ϕ_m) for the orientation of the direction of $g_{//}$ for site A in the lattice, calculated from the EPR data.

$(g^2)_{xx}$	4.2431(7)	$(g^2)_{xy}$	0.0229(3)
$(g^2)_{yy}$	5.1491(3)	$(g^2)_{zx}$	0.0148(1)
$(g^2)_{zz}$	4.2073(9)	$(g^2)_{zy}$	0.0243(6)
$(g^2)_1$	4.2018(1)	$\boldsymbol{a_1}$	[0.330(1) 0.016(5)−0.944(5)]
$(g^2)_2$	4.2475(3)	$\boldsymbol{a_2}$	[0.944(5)−0.0 33(5) 330(1)]
$(g^2)_3$	5.1503(6)	$\boldsymbol{a_3}$	[0.026(5) 1 0.026(5)]
$g_\perp$	2.0489(3)	θ_m	90.27°
$g_{//}$	2.2794(9)	ϕ_m	−89.72°

$$\kappa(x) = \frac{1}{N_s x}\langle S_z^2 \rangle = \frac{0.05066 - 0.02380x + 0.11360x^2 - 0.09830x^3 + 0.30900x^4}{1 - 0.08517x + 1.51000x^2 + 1.12480x^3 + 0.85950x^4 + 1.23650x^5} \quad (5)$$

Values $2J = -0.32(2)\ cm^{-1}$ and $g = 2.07(2)$ were obtained for the exchange parameter and the g-factor by fitting Eqs. (4) and (5), to the susceptibility data in Fig. 3a. We also calculated $2J = -0.28(5)\ cm^{-1}$ and $g = 2.070(5)$ fitting Eq. (2) to the isothermal magnetization curve in Fig. 3b. The curves calculated with these values agree well with the data. The values of $2J$ obtained from the susceptibility and the magnetization are in reasonable agreement and we set an average value $2J = -0.30(2)\ cm^{-1}$.

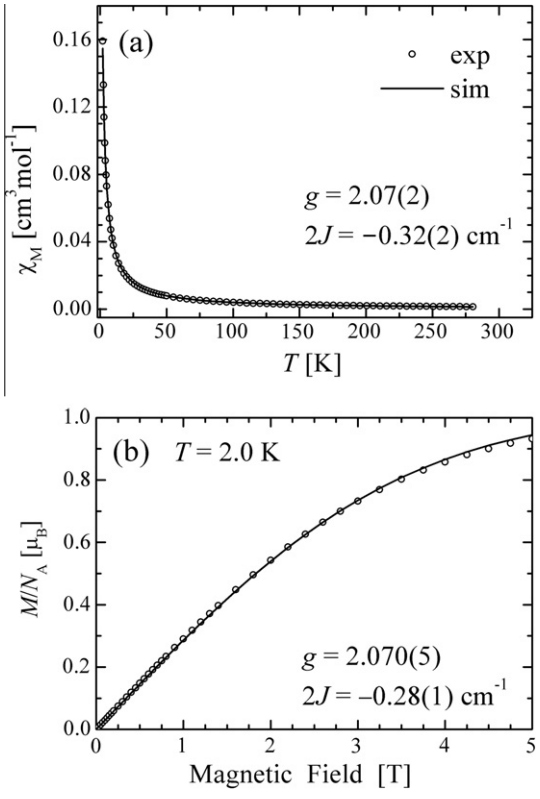

Fig. 3. (a) Temperature dependence of the magnetic susceptibility. (b) Isothermal magnetization curve observed at $T = 2$ K. Symbols are experimental values. Solid lines are calculations explained in the text.

3.4. EPR results

The EPR spectrum at 34.0 GHz of a powder sample of $[Cu(lys)Cl_2]$ (not shown) is typical of Cu^{II} ions in axial symmetry sites of paramagnetic materials. The absence of hyperfine splitting, that is washed out by the couplings between copper spins [54,55], is expected because the hyperfine parameter $|A| \sim 0.01\ cm^{-1}$ is much smaller than the nearest neighbor exchange coupling $|2J|$. The powder spectrum was fitted using the EasySpin program [56] and the optimization routines provided by Matlab [57] as described by Gerard et al. [58], assuming that the principal axes of the g-matrix and those of the angular variation of the line width are the same, to obtain $g_1 = 2.067$, $g_2 = 2.074$ and $g_3 = 2.257$. The simulated spectrum is in good agreement with the observed spectrum.

According to the lattice structure of $[Cu(lys)Cl_2]$ there are Cu molecules in two orientations related by a C_2 rotation around $\boldsymbol{b}$ which should give rise to two symmetry related EPR lines for most

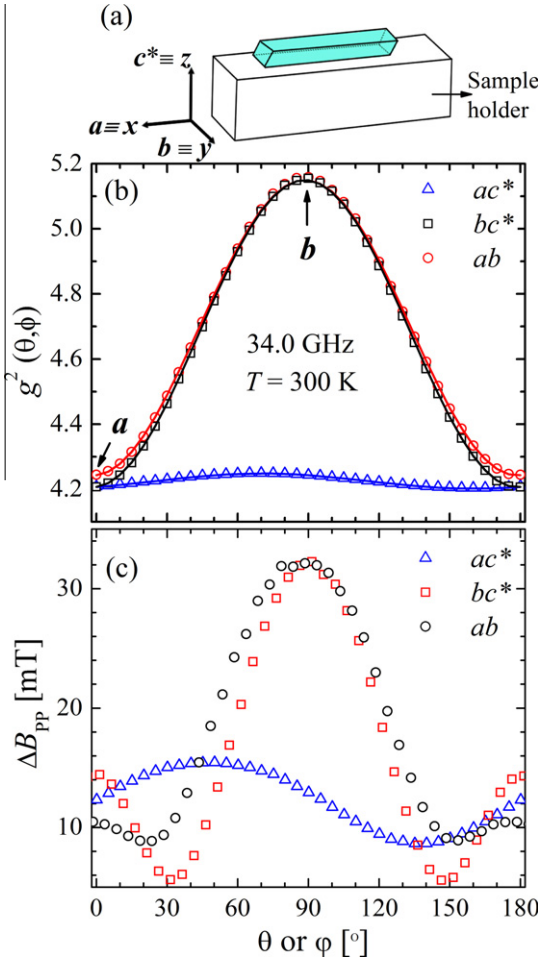

Fig. 4. (a) Mounting of the samples on a KBr holder for the EPR measurements. The positions of the crystal axes *a*, *b* and $c^* = a \times b$ in the *xyz* axes of the holder are indicated. (b) Angular variation of the squared g-factor $g^2(\theta, \phi)$ in the planes *ab*, *ac**, *bc**. The symbols are the experimental values. The solid lines were obtained with the components of the ***g*·*g*** matrix given in Table 3. (c) Angular variation of the peak−to−peak line width ΔB_{PP} observed in the *ab*, *bc** and *ac** crystal planes.

magnetic field orientations [59]. The single line observed for the magnetic field in the three crystallographic planes of a single crystal sample arises from the exchange interaction 2*J* between neighboring Cu^{II} ions which is large enough to collapse these resonances and the unobserved hyperfine coupling [60,61]. The experimental values for $g^2(\theta, \phi)$ (where θ and ϕ define the magnetic field orientation) are displayed in Fig. 4a and the result can be described with the spin-Hamiltonian:

$$\mathcal{H} = \mu_B \boldsymbol{S} \cdot \boldsymbol{g} \cdot \boldsymbol{B}_0 \quad (6)$$

In Eq. (6) μ_B is the Bohr magneton, $\boldsymbol{S}$ is the effective spin operator ($S = ½$), $\boldsymbol{g}$ is the crystal *g*-matrix, defined as the average of the molecular $\boldsymbol{g_i}$ matrices (i = A, B, C, D), and $\boldsymbol{B_0} = B_0 h$, where $\boldsymbol{h} = \boldsymbol{B_0}/|\boldsymbol{B_0}| = (\sin\theta\cos\phi, \sin\theta\sin\phi, \cos\theta)$. The components of the $\boldsymbol{g^2}$-matrix obtained by fitting the function $g^2(\theta, \phi) = \boldsymbol{h\,g\,g\,h}$ to the data are given in Table 3 with its eigenvalues and eigenvectors. The solid lines in Fig. 4a, calculated with these parameters, are in good agreement with the data.

We evaluated the molecular $\boldsymbol{g}_i$-matrices of the individual copper ions from the crystal *g*-matrix following the procedure described by Calvo and Mesa [62]. Since the coordination around the copper ion is approximately square planar, we assume axial symmetry, and obtained $g_{//}$, $g_\perp$, and the orientation angles (θ_m, ϕ_m) for the axial direction, included in Table 3. These angles are in good agreement with the crystallographic results ($\theta_{cris} = 90.80°$, $\phi_{cris} = -89.20°$), supporting the axial symmetry assumed in the calculation and indicating a $d(x^2 - y^2)$ ground orbital state.

The peak-to-peak line width $\Delta B_{pp}(\theta, \phi)$ of the resonance observed as a function of the orientation of $\boldsymbol{B_0}$ in the *ab*, *ac** and *bc** planes (Fig. 4b) has a maximum value 32 mT along the chain axis ***b*** in the *ab* and *bc** planes and minima of 5.6 mT at $\theta = 30.0°$ and 145.0° in the *bc** plane. In the *ab* and *bc** planes it displays a second maximum at 90° of the chain axis. This symmetry allows attributing the widths to magnetic dipolar interactions between copper ions, narrowed by the exchange couplings [2,53,63]. The behavior of the peak-to-peak line width in the three orthogonal planes results from the one-dimensional magnetic behavior.

Table 4
Magnetic and structural data for $[Cu(lys)Cl_2]$ and related compounds. The angles φ and δ are defined in Fig. 1.

Compound	Cu−Cl distance (Å)		Cu−Cu distance (Å)	φ (°)	δ (°)	φ/R	$2J$ (cm^{-1})	Factor-*g*	References
	Short	Long (*R*)							
$[Cu(lys)Cl_2]$	2.3021(12)	2.879(2)	3.5414(4)	85.48(6)	171.29(13)	29.7	−0.30(2)	$g_1 = 2.2694$ $g_2 = 2.0498$ $g_3 = 2.0609$	this work
$Cu(imH)_2Cl_2$	2.365(4)	2.751(6)	4.37	117		42.5	−2.1	$g_1 = 2.24(1)$ $g_2 = 2.09(1)$ $g_3 = 2.03(1)$	[12]
cis-$[Cu(maep)Cl_2]$	2.300(2)	2.785(2)	4.263(2)	113.6(5)	165.7(1)	40.8	1.58		[13]
$Cu(dmso)_2Cl_2$	2.290(2)	2.702(2)	4.757(2)	144.6(1)	146.1(9)	53.5	−6.1		[13]
$[Cu(paphy)Cl](PF)_6$	2.217(4)	2.805(4)	3.919(3)	102.3(2)	161.3(9)	36.5	0.63	$g_{//} = 2.200$ $g_\perp = 2.045$	[15]
$[CuCl_2(TzHy)]$	2.244(1)	2.994(2)	3.996(1)	97.4(1)	162.1	32.5	−8.6	$g = 2.148(6)$	[16]
$[Cu(pepci)Cl](PF)_6$	2.265(7)	2.797(8)	4.766(5)	137.6(3)	156.0(5)	49.2	−1.39	$g_{//} = 2.219$ $g_\perp = 2.059$	[17]
$[\{LCuIICl\}(\mu\text{-benzoato})](ClO_4)$	2.327(2)	2.872(3)	3.565(2)	85.9(2)	176.8(2)	29.9	−1.2	$g = 2.24$	[18]
$Cu(bipy)Cl_2$	2.291(3)	2.674(3)	4.01	107.50(10)	158.5(2)	40.2	−2.3		[19]
1/n$[Cu(HL)Cl]_n$	2.2643(4)	2.8343(4)	4.429	103.08(1)	174.10(4)	36.6	−0.5(1)	$g = 2.11(1)$	[20]
$[Cu(dpg)Cl_2]$	2.247(2)	2.904(2)	3.649(1)	89.3		30.7	−0.85(1)		[32]

Abbreviations: imH = imidazole; maep = 2-(2′-methylaminoethyl)pyridine; dmso = dimethylsulphoxide; paphy = pyridine-2-carboxaldehyde 2-pyridylhydrazone; pepci = N-(2-pyridylethyl)pyridine-2-carbaldimine; bipy = 2,2'-bipyridine; HL = 3-(2-(Methylthio)phenylazo)-2,4-pentanedione; L = 1,4,7-trimethyl-1,4,7-triazacyclonane; dpg = diphenylgyloximate, TzHy = (4,5-dihydro-1,3-thiazol-2-yl)hydrazine. Lundberg [12] define the Hamiltonian $\mathcal{H}_{ex}(i,j) = -J\boldsymbol{S}_i\boldsymbol{S}_j$, thus we changed their result according our definition.

4. Magneto structural-correlations

The exchange coupling 2*J* between copper ions depends on the bridging angles Cu–Cl–Cu and Cl–Cu–L_t (L_t-ligand trans to Cl), labeled φ and δ in Fig. 1, and on the length *R* of the axial Cu–Cl bond, determined by the structure of the Cu^{II} polyhedra [11,14–18]. Table 4 shows the values of 2*J* and these structural parameters for [Cu(lys)Cl_2] and for related compounds reported by other authors. It was noted by Cortés et al. [17], that a decrease of δ from 180° to 120°, corresponding to a change of the Cu^{II} coordination from square-pyramidal to trigonal–bipyramidal, favors stronger antiferromagnetic interactions as can be observed in Table 4, and that increase of φ from 90° also favors the antiferromagnetic interactions. Hatfield et al. [30] introduced the parameter φ/R to correlate the coupling and Table 4 also compares the values of φ/R and 2*J* for compounds containing a single Cu–Cl–Cu bridge. [Cu(lys)Cl_2] has the smallest angle φ, and the longest *R* bond distance among all known mono-chloride-bridged copper chains, a characteristic that explains the relatively small exchange coupling found in this compound. One also observes this correlation for the structural parameters and 2*J* values for [{$LCu^{II}Cl$}(μ-benzoato)](ClO_4) [18] and Cu(dpg)Cl_2 [32] (Table 4). In general, the values of 2*J* vary from −8.6 to 1.58 cm^{-1} while the φ/R ratio increases from 29.6 to 53.5, revealing that the larger φ/R ratio produces a ferromagnetic character, in agreement with Hatfield's hypothesis. This correlation can also be observed analyzing the 2*J* values against the bridging angle φ, when smaller values of φ in monochloro Cu^{II} chains are associated with a decrease of 2*J* [13,14].

Considering our structural, EPR and magnetic results for [Cu(lys)Cl_2], and the trends proposed by Cortés et al. [17] and Marsh et al. [30], one predicts a $d(x^2-y^2)$ ground state orbital in the basal plane of Cu^{II} ions, and justify the weak antiferromagnetic exchange interaction 2*J* as due to a vanishing effective overlapping between the $d(x^2-y^2)$ orbitals of adjacent Cu^{II} ions in the chains [64]. Indeed, Llobet et al. [65] reported recently molecular orbital calculations based on the extended Hückel model for ideal coordination environment with parallel basal planes, showing that the magnetic interaction between adjacent square-pyramidal Cu^{II} centers are mainly mediated through π^* interactions between the $d(x^2-y^2)$ orbitals and the apical chloride *p* orbitals, which results in the weak magnetic coupling shown by our results. However, since various structural factors influence the magnitude of the exchange interaction 2*J*, its magnitude cannot be described by a simple formula.

5. Conclusions

We studied the synthesis, crystal structure and performed magnetic and EPR measurements for a new Cu^{II} compound with the amino acid L-lysine·HCl, in which the Cu^{II} ions are in polymeric chains bridged by monomeric chlorine bridges having the smallest Cu–Cl2–Cu angle and an unusually long Cu–Cl_{ap} bond for systems with single chlorine bridges. Our magnetic measurements allow evaluating a weak antiferromagnetic exchange coupling between Cu^{II} ions and the components of the *g*-matrix obtained from the EPR spectra that are explained in terms of the characteristics of the superexchange bridges and the properties of the Cu^{II} site.

Acknowledgements

The authors thank Dr. E.E. Castellano (Instituto de Física de São Carlos – USP) for allowing us to use his KappaCCD X-ray diffractometer. This work was supported by CNPq, CAPES, FUNAPE and FAPEG in Brazil and by CAI+D-UNL in Argentina. R.C. is a member of CONICET.

Appendix A. Supplementary data

CCDC 889314; contains the supplementary crystallographic data for [Cu(lys)Cl_2]. These data can be obtained free of charge via http://www.ccdc.cam.ac.uk/conts/retrieving.html, or from the Cambridge Crystallographic Data Centre, 12 Union Road, Cambridge CB2 1EZ, UK; fax: (+44) 1223 336 033; or e-mail: deposit@ccdc.cam.ac.uk. Supplementary data associated with this article can be found, in the online version, at http://dx.doi.org/10.1016/j.poly.2012.08.045.

References

[1] Y. Shimazaki, M. Tajani, O. Yamauchi, Dalton Trans. (2009) 7854.
[2] R. Calvo, Appl. Magn. Reson. 31 (2007) 271.
[3] E.I. Solomon, K.W. Penfield, D.E. Wilcox, Struct. Bond. 53 (1983) 1.
[4] K.W. Penfield, R.R. Gay, R.S. Himmelwright, N.C. Eickman, V.A. Norris, H.C. Freeman, E.I. Solomon, J. Am. Chem. Soc. 103 (1981) 4382.
[5] B. Abolmaali, H.V. Taylor, U. Weser, Struct. Bond. 91 (1998) 91.
[6] K.D. Karlin, Z. Tyeklar, Bioinorganic Chemistry of Copper, Chapman and Hall, New York, 1993.
[7] S.H. Laurie, G. Wilkinson, R.D. Gillard, J.A. Mc Cleverty (Eds.), Comprehensive Coordination Chemistry, vol. 2, Pergamon Press, Oxford, 1987. pp. 739–776.
[8] (a) R. Calvo, P.R. Levstein, E.E. Castellano, S.M. Fabiane, O.E. Piro, S.B. Oseroff, Inorg. Chem. 30 (1991) 216;
(b) R. Calvo, M.C.G. Passeggi, M.A. Novak, O.G. Symko, S.B. Oseroff, O.R. Nascimento, M.C. Terrile, Phys. Rev. B 43 (1991) 1074;
(c) C.D. Brondino, N.M.C. Casado, M.C.C. Passeggi, R. Calvo, Inorg. Chem. 32 (1993) 2078;
(d) R. Calvo, C.A. Steren, O.E. Piro, T. Rojo, F.J. Zuñiga, E.E. Castellano, Inorg. Chem. 32 (1993) 6016;
(e) R.E. Rapp, E.P. de Souza, H. Godfrin, R. Calvo, J. Phys. Condens. Mat. 7 (1995) 9595;
(f) R. Calvo, M.C.G. Passeggi, N.O. Moreno, G.E. Barberis, A. Braun Chaves, B.C.M. Torres, L. Lezama, T. Rojo, Phys. Rev. B 60 (1999) 1197.
[9] G.E. Schulz, R.H. Schrimer, in: R.H. Cantor (Ed.), Principles of Protein Structure, Springer-Verlag, New York, 1990.
[10] J.D. Dunitz, Acta Cryst. 10 (1957) 307.
[11] J.A.C. van Ooijenand, J. Reedijk, J. Chem. Soc. Dalton Trans. (1978) 1170.
[12] B.K.S. Lundberg, Acta Chem. Scand. 26 (1972) 3977.
[13] W.E. Estes, W.E. Hatfield, J.A.C. van Ooijenand, J. Reedijk, J. Chem. Soc. Dalton Trans. (1980) 2121.
[14] C.P. Landee, R.E. Greeney, Inorg. Chem. 25 (1986) 3771.
[15] T. Rojo, J.M. Mesa, M.I. Arriortua, J.M. Savariault, J. Galy, G. Villeneuve, D. Beltrán, Inorg. Chem. 27 (1988) 3904.
[16] F.J. Barros-García, A. Bernalte-García, F.J. Higes-Rolando, F. Luna-Giles, A.M. Pizarro-Galán, E. Viñuelas-Zahínos, Z. Anorg, Allg. Chem. 631 (2005) 1898.
[17] R. Cortés, L. Lezama, J.I.R. Larramendi, G. Madariaga, J.L. Mesa, F.J. Zuñiga, T. Rojo, Inorg. Chem. 34 (1995) 778.
[18] K.-S. Bürger, P. Chaudhuri, K. Wieghardt, Inorg. Chem. 35 (1996) 2704.
[19] M. Hernández-Molina, J. González-Platas, C. Ruiz-Pérez, F. Lloret, M. Julve, Inorg. Chim. Acta 284 (1999) 258.
[20] M.K. Paira, T.K. Mondal, E. López-Torres, J. Ribas, C. Sinha, Polyhedron 29 (2010) 3147.
[21] S.S. Roberts, D.R. Bloomquist, R.D. Willett, H.W. Dodgen, J. Am. Chem. Soc. 103 (1981) 2603.
[22] S.K. Hoffmann, D.J. Hodgson, W.E. Hatfield, Inorg. Chem. 24 (1985) 1194.
[23] M. Rodríguez, A. Llobet, M. Corbella, A.E. Martell, J. Reibenspies, Inorg. Chem. 38 (1999) 2328.
[24] (a) G.A. van Albada, S. Tanase, I. Mutikainen, U. Turpeinen, J. Reedijk, Inorg. Chim. Acta 361 (2008) 1463;
(b) G.A. van Albada, I. Mutikainen, U. Turpeinen, J. Reedijk, Inorg. Chim. Acta 362 (2009) 3373.
[25] S. Mandal, F. Lloret, R. Mukherjee, Inorg. Chim. Acta 362 (2009) 27.
[26] R.D. Willet, D. Gatteschi, O. Kahn (Eds.), Magneto-Structural Correlations in Exchange Coupled Systems, NATO ASI Series C, vol. 14, Reidel, Dordrecht, 1984.
[27] J.R. Friedman, M.P. Sarachik, J. Tejada, R. Ziolo, Phys. Rev. Lett. 76 (1996) 3830.
[28] L. Thomas, L. Lionti, R. Ballou, D. Gatteschi, R. Sessoli, B. Barbara, Nature 383 (1996) 145.
[29] S.G.N. Roundhill, D.M. Roundhill, D.R. Bloomquist, C. Landee, R.D. Willett, D.M. Dooley, H.B. Gray, Inorg. Chem. 18 (1979) 831.
[30] W.E. Marsh, W.E. Hatfield, D.J. Hodgson, Inorg. Chem. 21 (1982) 2679.
[31] W.E. Marsh, K.C. Pattel, W.E. Hatfield, D.J. Hodgson, Inorg. Chem. 22 (1983) 511.
[32] M. Mégnamisi-Bélombé, P. Singh, D.E. Bolster, W.E. Hatfield, Inorg. Chem. 23 (1984) 2578.
[33] J.S. Bonner, M.E. Fisher, Phys. Rev. A135 (1964) 640.
[34] W.A. Alves, R.H.A. Santos, A. Paduan-Filho, C.C. Becerra, A.C. Borin, A.M.C. Ferreira, Inorg. Chim. Acta 357 (2004) 2269.
[35] Bruker-Nonius, Kappa CCD Reference Manual, Nonius B.V., P.O. Box 811, 2600 Av., Delft, The Netherlands, 1998.

[36] Enraf-Nonius, Collect, Nonius BV, Delft, The Netherlands, 1997–2000.
[37] Z. Otwinowski, W. Minor, in: C.W. Carter Jr., R.M. Sweet (Eds.), Methods in Enzymology – Macromolecular Crystallography, Academic Press, New York, 1997, pp. 307–326.
[38] P. Coppens, in: F.R. Ahmed, S.R. Hall, C.P. Huber (Eds.), Crystallographic Computing, Copenhagen, Munksgaard, 1970, pp. 255–270.
[39] G.M. Sheldrick, SHELXS-97, Program for Crystal Structure Solution, University of Göttingen, Germany, 1997.
[40] G.M. Sheldrick, SHELXL-97, Program for Crystal Structure Refinement, University of Göttingen, Germany, 1997.
[41] L.J. Farrugia, J. Appl. Cryst. 30 (1997) 565.
[42] C.F. Macrae, I.J. Bruno, J.A. Chisholm, P.R. Edgington, P. McCabe, E. Pidcock, L. Rodriguez-Monge, R. Taylor, J. van de Streek, P.A. Wood, J. Appl. Cryst. 41 (2008) 466.
[43] L.J. Farrugia, J. Appl. Cryst. 32 (1999) 837.
[44] M.T.L.S. Duarte, M.A.A. de, C.T. Carrondo, M.L.S. Simões Gonçalves, M.B. Hursthouse, N.P.C. Walker, H.M. Dawes, Inorg. Chim. Acta 108 (1985) 11.
[45] L. Martinez, R.F. Farias, C. Airoldi, Termochim. Acta 395 (2003) 21.
[46] M.K. Marchewka, S. Debrus, H. Ratajczak, Cryst. Growth Des. 3 (2003) 587.
[47] A.W. Addison, T.N. Rao, J. Reedijk, J. van Rijn, G.C. Verschoor, J. Chem. Soc. Dalton Trans. (1984) 1349.
[48] B.J. Hathaway, G. Wilkinson, R.D. Gillard, J.A. McCleverty (Eds.), Comprehensive Coordination Chemistry, vol. 5, Pergamon Press, Oxford, UK, 1987.
[49] A.J. Costa-Filho, O.R. Nascimento, L. Ghivelder, R. Calvo, J. Phys. Chem. B 105 (2001) 5039.
[50] E.F. Chagas, R.E. Rapp, D.E. Rodrigues, N.M.C. Casado, R. Calvo, J. Phys. Chem. B 110 (2006) 8052.
[51] K. Fabricius, U. Löw, K.H. Mutter, P. Ueberholz, Phys. Rev. B 44 (1991) 7476.
[52] J.W. Hall, W.E. Marsh, R.R. Weller, W.E. Hatfield, Inorg. Chem. 20 (1981) 1033. See also, W.E. Hatfield, J. Appl. Phys. 52 (1981) 1985–1990.
[53] R.P. Sartoris, R.C. Santana, R.F. Baggio, O. Peña, M. Perec, R. Calvo, Inorg. Chem. 49 (2010) 5650.
[54] Z.G. Soos, J. Chem. Phys. 44 (1966) 1729.
[55] H.A. Farach, E.F. Strother, C.P. Poole, J. Phys. Chem. Solids 31 (1970) 1491.
[56] S. Stoll, A. Schweiger, J. Magn. Reson. 178 (2006) 42.
[57] Matlab, The Mathworks Inc., Natick, MA 01760.
[58] M.F. Gerard, C. Aiassa, N.M.C. Casado, R.C. Santana, M. Perec, R.E. Rapp, R. Calvo, J. Phys. Chem. Solids 68 (2007) 1533.
[59] J.M. Schveigkardt, A.C. Rizzi, O.E. Piro, E.E. Castellano, R.C. Santana, R. Calvo, C.D. Brondino, Eur. J. Inorg. Chem. (2002) 2913.
[60] P.W. Anderson, J. Phys. Soc. Jpn. 9 (1954) 316.
[61] R. Kubo, K. Tomita, J. Phys. Soc. Jpn. 9 (1954) 888.
[62] R. Calvo, M. Mesa, Phys. Rev. B 28 (1983) 1244.
[63] (a) P.R. Levstein, C.A. Steren, A.M. Gennaro, R. Calvo, Chem. Phys. 120 (1988) 449;
(b) P.R. Levstein, R. Calvo, Inorg. Chem. 29 (1990) 1581.
[64] P. Alemany, S. Alvarez, Inorg. Chem. 2 (1990) 723.
[65] M. Rodríguez, A. Llobet, M. Corbella, Polyhedron 19 (2000) 2483.